

The Observed Growth of Massive Galaxy Clusters III: Testing General Relativity on Cosmological Scales

David Rapetti^{1*}, Steven W. Allen¹, Adam Mantz^{1,2} and Harald Ebeling³

¹ *Kavli Institute for Particle Astrophysics and Cosmology at Stanford University, 452 Lomita Mall, Stanford 94305-4085, CA, USA and SLAC National Accelerator Laboratory, 2575 Sand Hill Road, Menlo Park 94025, CA, USA*

² *NASA Goddard Space Flight Center, Code 662, Greenbelt, MD 20771, USA*

³ *Institute for Astronomy, 2680 Woodlawn Drive, Honolulu, HI 96822, USA*

Accepted ???, Received ???; in original form 7 June 2018

ABSTRACT

This is the third of a series of papers in which we derive simultaneous constraints on cosmological parameters and X-ray scaling relations using observations of the growth of massive, X-ray flux-selected galaxy clusters. Our data set consists of 238 clusters drawn from the *ROSAT* All-Sky Survey, and incorporates extensive follow-up observations using the *Chandra* X-ray Observatory. Here we present improved constraints on departures from General Relativity (GR) on cosmological scales, using the growth index, γ , to parameterize the linear growth rate of cosmic structure. Using the method of Mantz et al. (2009a), we simultaneously and self-consistently model the growth of X-ray luminous clusters and their observable-mass scaling relations, accounting for survey biases, parameter degeneracies and the impact of systematic uncertainties. Such analysis of the survey and follow-up data is crucial, else spurious constraints may be obtained. We combine the X-ray cluster growth data with cluster gas mass fraction, type Ia supernova, baryon acoustic oscillation and cosmic microwave background data. We find that the combination of these data leads to a tight correlation between γ and the normalization of the matter power spectrum, σ_8 . Consistency with GR requires a measured growth index of $\gamma \sim 0.55$. Under the assumption of self-similar evolution and constant scatter in the cluster observable-mass scaling relations, and for a spatially flat model with a cosmological constant, we measure $\gamma(\sigma_8/0.8)^{6.8} = 0.55^{+0.13}_{-0.10}$, with allowed values for σ_8 in the range 0.79 to 0.89 (68.3 per cent confidence limits). Relaxing the assumptions on the scaling relations by introducing two additional parameters to model possible evolution in the normalization and scatter of the luminosity-mass relation, we obtain consistent constraints on γ that are only ~ 20 per cent weaker than those above. Allowing the dark energy equation of state, w , to take any constant value, we simultaneously constrain the growth and expansion histories, and find no evidence for departures from either GR or the cosmological constant plus cold dark matter paradigm. Our results represent the most robust consistency test of General Relativity on cosmological scales to date.

Key words: cosmological parameters – cosmology: observations – cosmology: theory – X-ray: galaxies: clusters

1 INTRODUCTION

Since Riess et al. (1998) and Perlmutter et al. (1999) first demonstrated, using observations of type Ia supernovae (SNIa), that the expansion history of the Universe is accelerating at late times, improved SNIa studies have continuously corroborated these results (Garnavich et al. 1998; Schmidt et al. 1998; Knop et al. 2003; Tonry et al. 2003;

Barris et al. 2004; Riess et al. 2004, 2007; Astier et al. 2006; Wood-Vasey et al. 2007; Kowalski et al. 2008; Hicken et al. 2009). At the same time, measurements of anisotropies in the cosmic microwave background (CMB) with the Wilkinson Microwave Anisotropy Probe (WMAP Spergel et al. 2003, 2007; Komatsu et al. 2009; Dunkley et al. 2009, and companion papers) and other CMB experiments (Readhead et al. 2004; Jones et al. 2006; Reichardt et al. 2009; Chiang et al. 2010; Gupta et al. 2009) have tightly constrained other key cosmological parameters. A variety

* Email: drapetti@slac.stanford.edu

of other cosmological data sets have also been used to independently measure cosmic acceleration. Measurements of the gas mass fraction (f_{gas}) in galaxy clusters, having earlier shown that the mean matter density of the Universe is low, $\Omega_m \sim 0.25$ (see e.g. White et al. 1993), have directly confirmed the effects of cosmic acceleration, at comparable significance to that seen in SNIa data (see e.g. Allen et al. 2004, 2008). Measurements of baryon acoustic oscillations (BAO) in galaxy surveys (see e.g. Eisenstein et al. 2005; Percival et al. 2007, 2010), the correlation of the low multipoles of the CMB with large scale structure observations from various surveys (see e.g. Scranton et al. 2003; Fosalba et al. 2003; Cabre et al. 2006; Giannantonio et al. 2008; Ho et al. 2008), and weak gravitational lensing by large scale structure (Schrabback et al. 2009) have also shown evidence for cosmic acceleration. The combination of subsets and/or all of these data have led to the establishment of the Λ CDM paradigm, in which the energy density of the Universe is currently composed of ~ 5 per cent baryons, ~ 20 per cent cold dark matter (CDM) and ~ 75 per cent dark energy, the last of which drives cosmic acceleration and has identical characteristics to Einstein's cosmological constant, Λ .

Together, the above experiments robustly show that the Universe is accelerating. However, the ability of such data to probe the underlying cause of this acceleration is limited. All of the above constraints on dark energy are primarily driven by its effects on the background geometry. Such data alone cannot distinguish acceleration due to a true dark energy component with negative pressure from modifications to the standard theory of gravity, i.e. Einstein's General Relativity (GR). Recently, however, Mantz et al. (2008, 2009a, hereafter Paper I), and Vikhlinin et al. (2009) have presented new constraints on dark energy from measurements of the growth of cosmic structure, as evidenced in X-ray flux-selected cluster samples. These experiments are sensitive not only to the evolution of the mean energy density background, but also to the evolution of the density perturbations with respect to this background. This work has provided clear, independent confirmation of the effects of dark energy in slowing the growth of X-ray luminous galaxy clusters.

The observed evolution of density perturbations provides a sensitive probe of the underlying theory of gravity and the clustering¹ properties of dark energy. Rapetti et al. (2009, hereafter R09) exploited this sensitivity to constrain departures from the predicted cosmic growth rate for GR using the convenient parameterization $\Omega_m(z)^\gamma$, for which GR has $\gamma \sim 0.55$ (Peebles 1980; Wang & Steinhardt 1998; Linder 2005; Huterer & Linder 2007; Di Porto & Amendola 2008; Sapone & Amendola 2007; Gannouji & Polarski 2008; Wei 2008; Linder & Cahn 2007; Nesseris & Perivolaropoulos 2008). Using the growth of structure analysis of Mantz et al. (2008), R09 found no evidence for deviations from either GR or Λ CDM. Recent results from the combination of

other cosmological data sets are also consistent with GR (Daniel et al. 2010; Zhao et al. 2010; Reyes et al. 2010).

This is the third of a series of papers in which, for the first time, we employ a fully self-consistent analysis of the growth of massive clusters that combines current X-ray cluster surveys and deep, pointed, follow-up observations to simultaneously constrain both cosmological parameters and observable-mass (luminosity-mass and temperature-mass) scaling relations. Importantly, the improved method, which is described in Paper I, properly accounts for all selection biases, covariances and parameter degeneracies, and models fully the impact of systematic uncertainties. Here, we utilize this improved method (hereafter XLF, as defined in Paper I) to re-investigate the simultaneous constraints that can be placed on γ and the background evolution (expansion history). For the background, we use two reference expansion models: flat Λ CDM, parameterized by the mean matter density, Ω_m ; and flat w CDM, parameterized by Ω_m and a constant dark energy equation of state, w . Our constraints on γ arise primarily from the XLF experiment, which uses the cluster samples of Ebeling et al. (1998, *ROSAT* Brightest Cluster Sample; BCS), Böhringer et al. (2004, *ROSAT*-ESO Flux Limited X-ray sample; REFLEX), Ebeling et al. (2001, 2009 in preparation, Bright MASSive Cluster Survey; Bright MACS), plus extensive X-ray follow-up data from the *Chandra* X-ray Observatory and *ROSAT* (for details see Mantz et al. 2009b, hereafter Paper II), although we also utilize the (currently) small additional constraining power available from measurements of the Integrated Sachs-Wolfe (ISW) effect at low multipoles in the CMB.

We emphasize that the models used for the evolution of the background and density perturbations are purely phenomenological, encompassing both modified gravity and clustering dark energy as possible sources for cosmic acceleration. Our analysis allows for a simple, but elegant test for departures from the standard GR and Λ CDM paradigms. Using the combination of XLF, f_{gas} , SNIa, BAO and CMB, we demonstrate good agreement with the standard GR+ Λ CDM model and provide tight constraints on the model parameters. We show that our results are robust against reasonable assumptions regarding the evolution of galaxy cluster scaling relations. We stress that in order to obtain robust results from current and future XLF studies, it is essential to employ a consistent analysis method, such as the one used here (see details in Paper I), in order to properly account for selection biases, covariances, parameter degeneracies and systematic uncertainties. Otherwise, spuriously tight constraints may be obtained.

2 COSMOLOGICAL MODEL

2.1 Linear growth rate

Galaxy clusters are the largest and rarest virialized objects in the Universe. Their abundance as a function of redshift provides an extremely sensitive probe of the underlying cosmology. To predict the cumulative number density of galaxy clusters, $n(M, z)$, at a given mass, M , and redshift, z , we calculate the evolution of density fluctuations using linear perturbation theory, accounting for non-linear effects using results from N-body simulations.

¹ Note that for models other than the cosmological constant, dark energy is expected to couple with gravity, i.e. cluster (see e.g. Hu 2005; Mota et al. 2007). For specific dark energy and modified gravity models, see the reviews of Copeland et al. (2006) and Frieman et al. (2008).

The cumulative mass function of dark matter halos can be calculated as

$$n(M, z) = \int_0^M f(\sigma) \frac{\bar{\rho}_m}{M'} \frac{d \ln \sigma^{-1}}{dM'} dM', \quad (1)$$

where $\bar{\rho}_m$ is the mean comoving matter density, σ^2 is the variance of the linearly evolved density field (as defined in Equation 5), and $f(\sigma)$ is a fitting formula obtained from theory or N-body simulations (Press & Schechter 1974; Bond et al. 1991; Sheth & Tormen 1999; Jenkins et al. 2001; Evrard et al. 2002). Remarkably, $f(\sigma)$ encompasses linear and non-linear effects in such a way that its form is approximately independent of the cosmology assumed (see Section 2.3).

Modifications to GR at large scales have been proposed as alternatives to dark energy to explain cosmic acceleration at late times. In general, in addition to changing the expansion history, such modifications also affect the growth of cosmic structure. As in R09, we parameterize the growth rate, $f(a)$, using (Peebles 1980; Wang & Steinhardt 1998; Linder & Cahn 2007)

$$f(a) \equiv \frac{d \ln \delta}{d \ln a} = \Omega_m(a)^\gamma, \quad (2)$$

where $\Omega_m(a) = \Omega_m a^{-3}/E(a)^2$. Here, Ω_m is the present, mean matter density in units of the critical density, $E(a) = H(a)/H_0$ the evolution parameter, $H(a)$ the Hubble parameter (with H_0 its present-day value), and γ the growth index.

We calculate the evolution of the linear matter density contrast, $\delta \equiv \delta\rho_m/\bar{\rho}_m$, i.e. the ratio of matter density fluctuations to the cosmic mean, by solving Equation 2. As an initial condition for this differential equation, we match the value of δ at early times ($z_t = 30$) to that of GR. Given $\delta(z)$, we obtain the growth factor between z_t and z ,

$$D(z) \equiv \frac{\delta(z)}{\delta(z_t)}. \quad (3)$$

Note that $z_t = 30$ is well within the dark matter dominated era, when the expansion is expected to be decelerating. At this time $f(a)$ is close to 1, independent of γ . Using $D(z)$, we calculate the linear matter power spectrum for a given wavenumber, k , and redshift,

$$P(k, z) \propto k^{n_s} T^2(k, z_t) D(z)^2, \quad (4)$$

where $T(k, z_t)$ is the matter transfer function of GR at redshift z_t , and n_s the primordial scalar spectral index. Given $P(k, z)$, the variance of the linearly evolved density field, smoothed by a spherical top-hat window function of comoving radius R enclosing mass $M = 4\pi\bar{\rho}_m R^3/3$, is then

$$\sigma^2(M, z) = \frac{1}{2\pi^2} \int_0^\infty k^2 P(k, z) |W_M(k)|^2 dk, \quad (5)$$

where $W_M(k)$ is the Fourier transform of the window function. Using this value for $\sigma(M, z)$ in Equation 1, we obtain $n(M, z)$.

2.2 Background evolution

Equation 2 depends on the evolution of the background energy density, through the parameter $E(a)$. Assuming an expansion history appropriate for Λ CDM, it has been shown (see e.g. Linder & Cahn 2007; Nesseris & Perivolaropoulos

2008) that, for $\gamma \sim 0.55$, the growth rate calculated using Equation 2 corresponds remarkably accurately to that predicted by GR. Linder & Cahn (2007) also showed that γ and w are only weakly correlated (see also R09) and, therefore, that one can measure the cosmic growth and expansion rates almost independently. These convenient properties of the γ -model provide us with a simple but powerful consistency test for GR.

Here, we perform this test using the new cluster XLF data (Papers I and II) in combination with f_{gas} , SNIa, BAO and CMB constraints. The latter four data sets primarily constrain the background evolution of the Universe, i.e. the expansion history. As a background expansion model, we use²

$$E(a) = \left[\Omega_m a^{-3} + (1 - \Omega_m) a^{-3(1+w)} \right]^{1/2}, \quad (6)$$

where w is the dark energy equation of state parameter and $w = -1$ corresponds to flat Λ CDM. Note that we use this model *only* as a phenomenological description of the expansion history. We do *not* assume the existence of dark energy. Our model allows us to simultaneously test for departures from Λ CDM in the expansion history ($w \neq -1$) and departures from GR in the growth history ($\gamma \neq 0.55$). Deviations from these benchmarks can be caused either by clustering dark energy or modified gravity.

2.3 Non-linear model

The fitting formula $f(\sigma)$ from Jenkins et al. (2001) has been tested for a wide range of background dark energy cosmologies and has been shown to provide a ‘‘universal’’ description, within ~ 20 per cent uncertainty (see e.g. Kuhlen et al. 2005; Lokas et al. 2004; Klypin et al. 2003; Linder & Jenkins 2003; Mainini et al. 2003; Maccio et al. 2004; Francis et al. 2009; Grossi & Springel 2009)³. However, in these tests, typically only the background evolution was modified, while the linear density perturbations of the new component (dark energy) were neglected. Recently, Jennings et al. (2010) have presented results that account for the effects of the density fluctuations provided by quintessence models on the linear matter power spectrum, finding only a small effect on $f(\sigma)$ for the masses and redshifts relevant here.

² R09 examined three expansion models: flat Λ CDM, flat w CDM and non-flat Λ CDM. For the latter, they found that there is negligible covariance between Ω_k , the curvature energy density, and γ . Since this test is computationally expensive, we do not repeat it here.

³ Schmidt et al. (2009) explored an $f(R)$ gravity model and showed that for values of their model parameter compatible with Solar Systems tests ($f_{R0} \sim 10^{-6}$), the halo mass function is in agreement with that of GR for very massive clusters (within the quoted level of uncertainty of the simulations). However, for more extreme values of the model parameter and for less massive clusters (for which chameleon effects are important), significant differences can arise. For the self-accelerating branch of the braneworld gravity model DGP (Dvali et al. 2000), Schmidt (2009a) and Chan & Scoccimarro (2009) predict a significant suppression of the halo mass function relative to GR, especially for massive objects. Schmidt (2009b) predicts an enhancement for the normal branch of this model.

The present study aims to test the consistency of current observations with GR (and Λ CDM). Therefore, we use an $f(\sigma)$ corresponding to GR, seeking to determine whether values of $\gamma \sim 0.55$ (and $w = -1$) are preferred by the data. Beyond the mass function of Jenkins et al. (2001), several authors have investigated the inclusion of an explicit dependence on redshift in the fitting formula $f(\sigma, z)$ (Lukić et al. 2007; Reed et al. 2007; Cohn & White 2008). Following Paper I, we use the $f(\sigma, z)$ function of Tinker et al. (2008), determined from a large suite of simulations,

$$f(\sigma, z) = A \left[\left(\frac{\sigma}{b} \right)^{-a} + 1 \right] e^{-c/\sigma^2}. \quad (7)$$

Here, parameters have the redshift dependence $x(z) = x_0(1+z)^{\varepsilon\alpha_x}$, with $x \in \{A, a, b, c\}$. The values for x_0 and α_x are given by Tinker et al. (2008). As described in Paper I, we use the parameter ε to account for residual systematic uncertainties in the evolution of $f(\sigma, z)$. We marginalize over the uncertainties in the parameters of Equation 7, accounting for their covariance. We also account for additional systematic uncertainties due to e.g. the presence of baryons (for details, see Paper I). Note, however, that, as we show in Paper I, the statistical and systematic uncertainties in $f(\sigma, z)$ are subdominant in the analysis. We have verified that ε is essentially uncorrelated with γ .

3 EVOLUTION OF THE SCALING RELATIONS

To compare the XLF data with the theoretical predictions of the mass function, we need to relate mass, M , to our observables: the X-ray luminosity, L , and average temperature, T , of the clusters. In Paper II, we describe the follow-up X-ray observations used to determine these relations. As discussed in Paper I, we simultaneously and self-consistently constrain both cosmological (see Section 2) and scaling relation parameters.

Following the notation of Paper II, we model the evolution of the luminosity-mass scaling relation as

$$\langle \ell(m) \rangle = \beta_0^{\ell m} + \beta_1^{\ell m} m + \beta_2^{\ell m} \log_{10}(1+z), \quad (8)$$

with a log-normal, and possibly evolving, intrinsic scatter of the luminosity at a given mass ⁴

$$\sigma_{\ell m}(z) = \sigma_{\ell m}(1 + \sigma'_{\ell m} z). \quad (9)$$

Here, $\ell \equiv \log_{10}[L_{500}E(z)^{-1}/10^{44} \text{ erg s}^{-1}]$ and $m \equiv \log_{10}[E(z)M_{500}/10^{15} M_{\odot}]$, where the subscript 500 refers to quantities measured within radius r_{500} , at which the mean, enclosed density is 500 times the critical density of the Universe at redshift z . The factors of $E(z)$ are required to account for the background evolution of the critical density. Fixing $\beta_2^{\ell m} = 0$, one has “self-similar” evolution of the scaling relation (Kaiser 1986; Bryan & Norman 1998), determined entirely by the $E(z)$ factors. Fixing $\sigma'_{\ell m} = 0$, one has constant scatter. In Paper II, we show that departures from self-similar evolution and evolution in $\sigma_{\ell m}(z)$ are not required by current data.

⁴ In the notation of R09, $\beta_0^{\ell m}$, $\beta_1^{\ell m}$, $\beta_2^{\ell m}$, $\sigma_{\ell m}$ and $\sigma'_{\ell m}$ correspond to $\log_{10}(M_0)$, β , ζ , η_0 and η_z , respectively.

In this paper we present results both for pure self-similarity and constant scatter ($\beta_2^{\ell m} = 0$, $\sigma'_{\ell m} = 0$), and also allowing for additional evolution in the luminosity-mass relation and its scatter, through $\beta_2^{\ell m}$ and $\sigma'_{\ell m}$. As we shall show, our improved analysis method (of Paper I) and the inclusion of high quality follow-up data for a significant fraction of clusters allows us to address even general questions of this type. We emphasize that for such analysis it is essential to *simultaneously* model the mass function, scaling relations, growth history and the impact of systematic uncertainties fully, else spurious constraints may be obtained.

The data and analysis of Paper I and II also include measured temperatures to simultaneously constrain the temperature-mass relation. In Paper II, we show that a simple power law

$$\langle t(m) \rangle = \beta_0^{tm} + \beta_1^{tm} m, \quad (10)$$

where $t \equiv \log_{10}(kT_{500}/\text{keV})$, without additional evolution parameters, such as β_2^{tm} and σ'_{tm} (which are defined equivalently to the corresponding parameters in the luminosity-mass relation, $\beta_2^{\ell m}$ and $\sigma'_{\ell m}$), is sufficient to describe the data. Note also that, for clusters with $kT > 3 \text{ keV}$, such as those used here, the flux within the 0.1 – 2.4 keV band is nearly independent of the temperature, and therefore β_2^{tm} and σ'_{tm} are essentially uncorrelated with γ .⁵ Thus, we do not further consider these parameters, and assume that the temperature-mass relation evolves self-similarly, with a constant log-normal scatter⁶.

4 ISW EFFECT

Our analysis also accounts for the small, but non-negligible additional constraining power on γ that is available from measurements from the ISW effect. The low multipoles of the CMB are sensitive to the growth of structure through this effect. The time-varying gravitational potentials of large scale structures contribute a net effect on the energy of the photons crossing them. For these photons, we calculate their contribution to the temperature anisotropy power spectrum as (Weller & Lewis 2003)

$$\Delta_l^{\text{ISW}}(k) = 2 \int dt e^{-\tau(t)} \phi'_{j_l}[k(t-t_0)], \quad (11)$$

where t is the conformal time, τ the optical depth to reionization, $j_l(x)$ the spherical Bessel function for the multipole l , and ϕ' the conformal time variation of the gravitational potential. The latter can be calculated in terms of γ using the Poisson equation, $k^2\phi = -4\pi G a^2 \delta\rho_m$, as (R09)

$$\phi' = \frac{4\pi G a^2}{k^2} \mathcal{H} \delta\bar{\rho}_m [1 - \Omega_m(a)^\gamma], \quad (12)$$

where \mathcal{H} is the conformal Hubble parameter. Since we are performing a consistency test of GR, we assume that, as in GR, the contributions of the anisotropic stress and energy flux are negligible (for details on these terms see

⁵ We have explicitly verified this to be the case.

⁶ Our analysis includes a correlation parameter between the intrinsic scatters of the luminosity-mass and temperature-mass relations, $\rho_{\ell tm}$ (see details in Paper II).

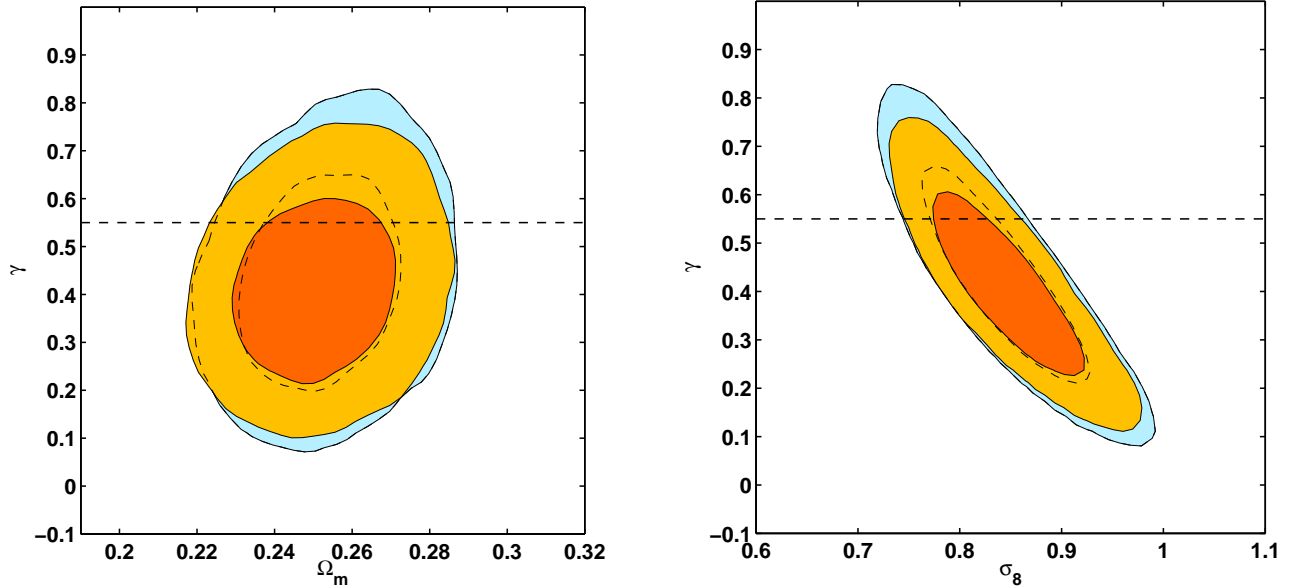


Figure 1. 68.3 and 95.4 per cent confidence contours in the Ω_m, γ (left panel) and σ_8, γ (right panel) planes for an assumed flat Λ CDM background model, using the combination of XLF, f_{gas} , SNIa, BAO and CMB data. The gold, smaller contours assume self-similar evolution of the observable-mass scaling relations and constant scatter ($\beta_2^{\ell m} = 0$; $\sigma'_{\ell m} = 0$). The blue, larger contours allow for departures from self-similarity and redshift evolution in the scatter of the luminosity-mass relation (Section 3; Paper II). The horizontal, dashed lines mark $\gamma = 0.55$, the growth index for GR.

Challinor & Lasenby 1999)⁷. As an initial condition, at $z = 2$ we match the $\Delta_l^{\text{ISW}}(k)$ to that of GR, using Equation 12 to evolve the model to $z = 0$. Unless stated, for results including CMB data, we include the constraints on γ available from the ISW effect.

5 DATA ANALYSIS

To constrain the cosmic growth rate we use three wide-area cluster samples drawn from the *ROSAT* all-sky survey: BCS ($z < 0.3$; northern sky; $F_X(0.1 - 2.4 \text{ keV}) > 4.4 \times 10^{-12} \text{ erg s}^{-1} \text{ cm}^{-2}$), REFLEX ($z < 0.3$; southern sky; $F_X > 3.0 \times 10^{-12} \text{ erg s}^{-1} \text{ cm}^{-2}$), and Bright MACS ($0.3 < z < 0.5$; ~ 55 per cent sky coverage; $F_X > 2 \times 10^{-12} \text{ erg s}^{-1} \text{ cm}^{-2}$). In order to keep systematic uncertainties to a minimum, for all three surveys, we impose a lower luminosity cut of $2.5 \times 10^{44} h_{70}^{-2} \text{ erg s}^{-1}$ ($0.1 - 2.4 \text{ keV}$). For the BCS, this gives a total of 78 clusters; for REFLEX, 126 clusters; and for Bright MACS, 34 clusters. In total we have 238 clusters.

To constrain the background evolution we also use measurements of the gas mass fraction (f_{gas}) in 42 massive, dynamically relaxed clusters from Allen et al. (2008), as well as the compilation of 307 SNIa from Kowalski et al. (2008), and BAO data (Percival et al. 2007; Colless et al. 2001, 2003; Adelman-McCarthy et al. 2007). The latter constrain the ratio of the sound horizon to the distance scale at $z = 0.25$ and $z = 0.35$. We also use the five-year WMAP data (Dunkley et al. 2009; Komatsu et al. 2009, and companion papers).

⁷ For particular alternative gravity models such as DGP, these terms will not be negligible (Hu & Sawicki 2007) and the Poisson equation will need to be modified (Hu 2008).

We calculate the posterior probability distributions of all parameters using the Metropolis Markov Chain Monte Carlo (MCMC) algorithm, as implemented in the COSMOMC⁸ code of Lewis & Bridle (2002). We use a modified version of this code that includes additional modules to calculate the likelihood for our two cluster experiments: f_{gas} ⁹ (Rapetti et al. 2005; Allen et al. 2008) and the XLF (Paper I). For analyses without CMB data, we use standard Gaussian priors on both the present-day Hubble constant, $H_0 = 72 \pm 8 \text{ km s}^{-1} \text{ Mpc}^{-1}$ (Freedman et al. 2001), and the mean physical baryon density, $\Omega_b h^2 = 0.0214 \pm 0.0020$ (Kirkman et al. 2003), from Big Bang Nucleosynthesis studies. When including the CMB data, we do not use these priors.

When using CMB data, instead of H_0 we fit θ . The latter is the (approximate) ratio of the sound horizon at last scattering to the angular diameter distance, which, as shown by Kosowsky et al. (2002), is less correlated than H_0 with other parameters. In all analyses, in addition to H_0 or θ , and $\Omega_b h^2$, we fit for the mean physical dark matter density, $\Omega_c h^2$; the logarithm of the adiabatic scalar amplitude, $\ln(A_s)$ (which is related to σ_8)¹⁰; the growth index, γ ; and, when stated, the kinematical w parameter¹¹. For the analyses with CMB data, we also fit the optical depth to reionization, τ , the adiabatic scalar spectral index, n_s , and marginalize over the amplitude of the Sunyaev-Zel'dovich effect from galaxy clusters, $0 < A_{\text{SZ}} < 2$ (Spergel et al. 2007). For analyses

⁸ <http://cosmologist.info/cosmomc/>

⁹ http://www.stanford.edu/~drapetti/fgas_module/

¹⁰ σ_8^2 is the $z = 0$ variance in the density field at scales of $8h^{-1} \text{ Mpc}$ (see equation 5).

¹¹ Recall that we use w purely as a kinematic parameter, allowing us to model the cosmic expansion history conveniently.

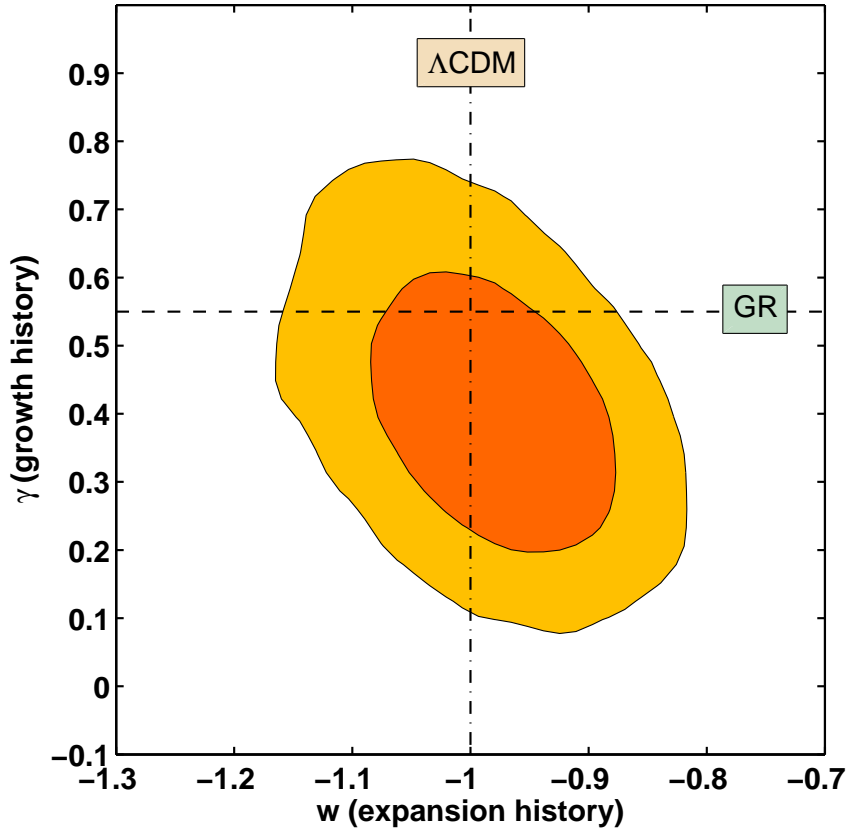


Figure 2. 68.3 and 95.4 per cent confidence contours in the w, γ plane for the flat w CDM background expansion model, using the combination of XLF, f_{gas} , SNIa, BAO and CMB data. The results assume self-similar evolution of the scaling relations and constant scatter ($\beta_2^{\ell m} = 0$; $\sigma'_{\ell m} = 0$). The horizontal, dashed line marks $\gamma = 0.55$, the growth history for GR. The vertical, dotted-dashed line marks $w = -1$, the expansion history for Λ CDM. The results are simultaneously consistent with GR and Λ CDM.

without CMB data, we fix n_s to 0.95 since, for such analyses, n_s is degenerate with σ_8 (see Paper I).

6 SIMULTANEOUS CONSTRAINTS ON THE GROWTH AND EXPANSION HISTORIES

6.1 Results for the Λ CDM expansion model

Figure 1 shows the joint constraints in the Ω_m, γ (left panel) and σ_8, γ (right panel) planes for a flat Λ CDM expansion history. The gold (smaller) contours show the constraints for the minimal, self-similar and constant-scatter scaling relation model ($\beta_2^{\ell m} = 0$ and $\sigma'_{\ell m} = 0$).

Figure 1 shows that, for the Λ CDM background model, Ω_m is not strongly correlated with γ . This supports the idea that γ is a useful parameterization to measure departures from the growth rate of GR, approximately independent of assumptions regarding the background evolution, parameterized in this case by Ω_m .

The right panel of Figure 1 shows a clear correlation between σ_8 and γ , with a correlation coefficient of $\rho = -0.87$. From the MCMC samples we measure $\gamma(\sigma_8/0.8)^{6.8} = 0.55^{+0.13}_{-0.10}$, with allowed values for σ_8 in the range $0.79 <$

$\sigma_8 < 0.89$ (marginalized 68.3 per cent confidence limits)¹². For $\sigma_8 = 0.8$, we measure $\gamma = 0.55$ (GR; marked by a horizontal, dashed line in Figure 1). Our results are consistent with GR at the 68.3 per cent confidence level. The observed correlation between σ_8 and γ shows that the addition of precise, independent knowledge of σ_8 should significantly improve the precision of the constraints on γ (see also Section 6.4).

The marginalized constraints on a single interesting parameter are summarized in Table 1.

6.2 Results for the w CDM expansion model

Figure 2 shows the joint constraints in the w, γ plane for the w CDM background cosmology (w constant), assuming self-similar evolution and constant scatter ($\beta_2^{\ell m} = 0$; $\sigma'_{\ell m} = 0$). The horizontal, dashed and vertical, dotted-dashed lines indicate $\gamma = 0.55$ (GR) and $w = -1$ (Λ CDM), respectively. Importantly, our results are simultaneously consistent with

¹² We calculate the exponent 6.8 finding the best constrained eigenvector for the estimated covariance matrix between $\ln \gamma$ and $\ln \sigma_8$.

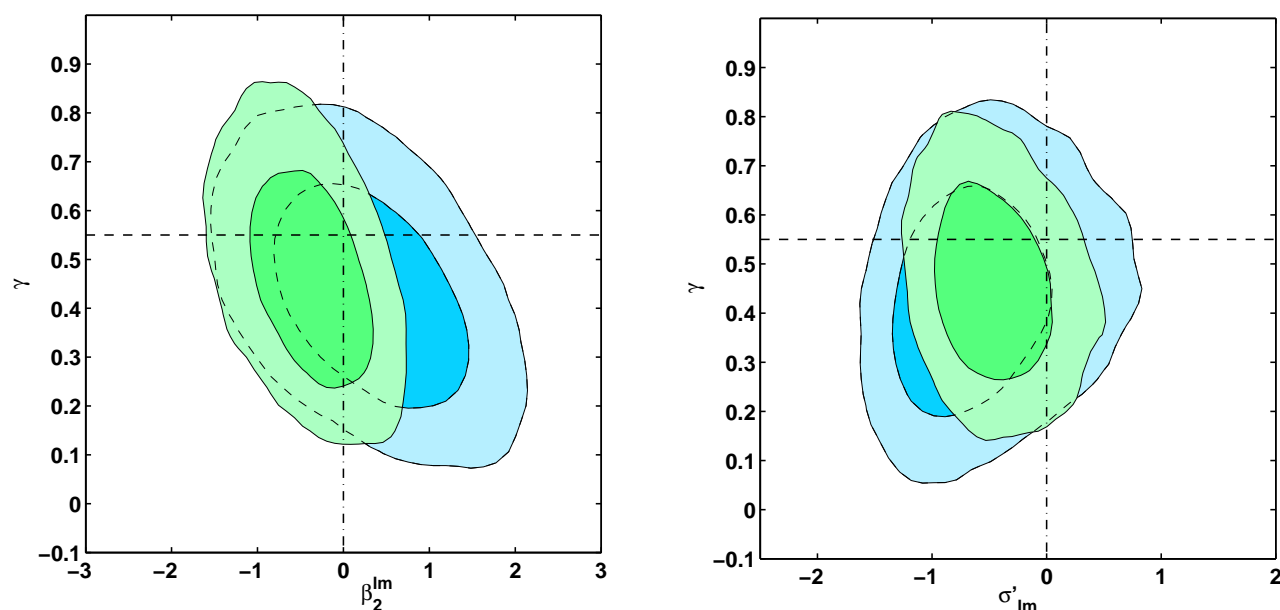


Figure 3. 68.3 and 95.4 per cent confidence contours in the $\beta_2^{\ell m}, \gamma$ (left panel) and $\sigma'_{\ell m}, \gamma$ (right panel) planes for the flat Λ CDM background evolution model, from the combination of XLF, f_{gas} , SNIa, BAO and CMB data. The green, smaller contours show the constraints obtained with either $\beta_2^{\ell m}$ (left panel) or $\sigma'_{\ell m}$ (right panel) allowed to be a free parameter. The blue, larger contours show the results when both parameters, $\beta_2^{\ell m}$ and $\sigma'_{\ell m}$, are allowed to be free. The horizontal, dashed lines mark $\gamma = 0.55$ (GR). The vertical, dotted-dashed lines mark the self-similar ($\beta_2^{\ell m} = 0$; left panel) and constant scatter ($\sigma'_{\ell m} = 0$; right panel) conditions.

both GR and Λ CDM at the 68.3 per cent confidence level (see Figure 2). For this expansion model, we again observe a correlation between σ_8 and γ , although somewhat less ($\rho = -0.69$) than for the Λ CDM case. The marginalized constraints on a single interesting parameters are summarized in Table 1.

6.3 Testing for departures from self-similarity

The blue (larger) contours in Figure 1 show the constraints obtained for the Λ CDM background model when allowing $\beta_2^{\ell m}$ and $\sigma'_{\ell m}$ to be free. Remarkably, using this (significantly) more complex model for the luminosity-mass relation, we obtain constraints on γ that are only ~ 20 per cent weaker than those for the minimal, self-similar, constant-scatter model (gold, smaller contours). The primary reason for this robustness is the comprehensive nature of the follow-up data in the XLF experiment, which tightly constrain the scaling relations and their evolution (Paper II).

Figure 3 shows the weak correlations between γ and the additional evolution parameters, $\beta_2^{\ell m}$ (left panel) and $\sigma'_{\ell m}$ (right panel). The blue (larger) contours in both panels are the constraints obtained with both parameters free; the green (smaller) contours show the results for models in which only a single additional parameter (either $\beta_2^{\ell m}$ or $\sigma'_{\ell m}$) is allowed to vary (fixing the other to 0; see also Table 1).

In Paper II, we show that, for GR models and a flat Λ CDM background, current X-ray data at $z < 0.5$ (survey+follow-up) do not require additional evolution of the scaling relations beyond the self-similar, constant scatter model (as implemented using the parameters $\beta_2^{\ell m}$, β_2^{tm} , $\sigma'_{\ell m}$ and σ'_{tm} ; see Section 3). Using the Deviance Information Criterion (DIC) of Spiegelhalter et al. (2002) (see defini-

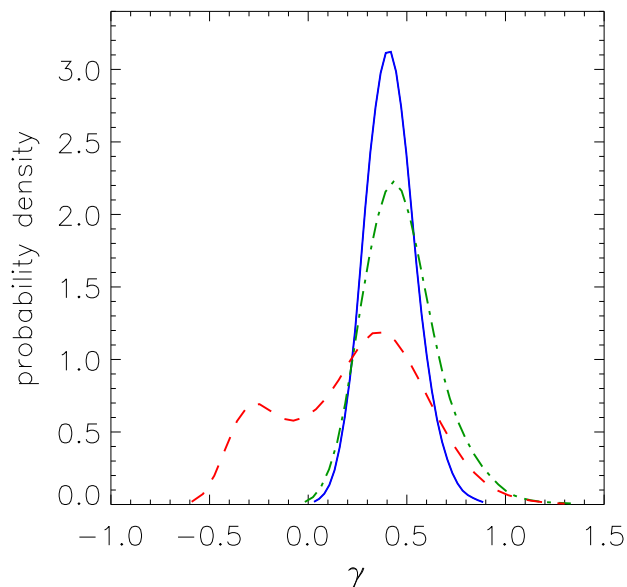


Figure 4. Marginalized constraints on γ for the flat Λ CDM background expansion model, from the XLF data alone (green, dotted-dashed line), from the combination of SNIa, f_{gas} , BAO and CMB data (red, dashed line), and from all the data sets combined, including the XLF (blue, solid line). It is clear that the XLF dominates the constraints on γ and that, alone, it provides significantly tighter constraints than those from the combination of the other data sets.

tion in Paper II) we have verified that the minimal model ($\beta_2^{\ell m} = 0$, $\sigma'_{\ell m} = 0$) remains an adequate description of the data, when γ is included as a parameter in the analysis.

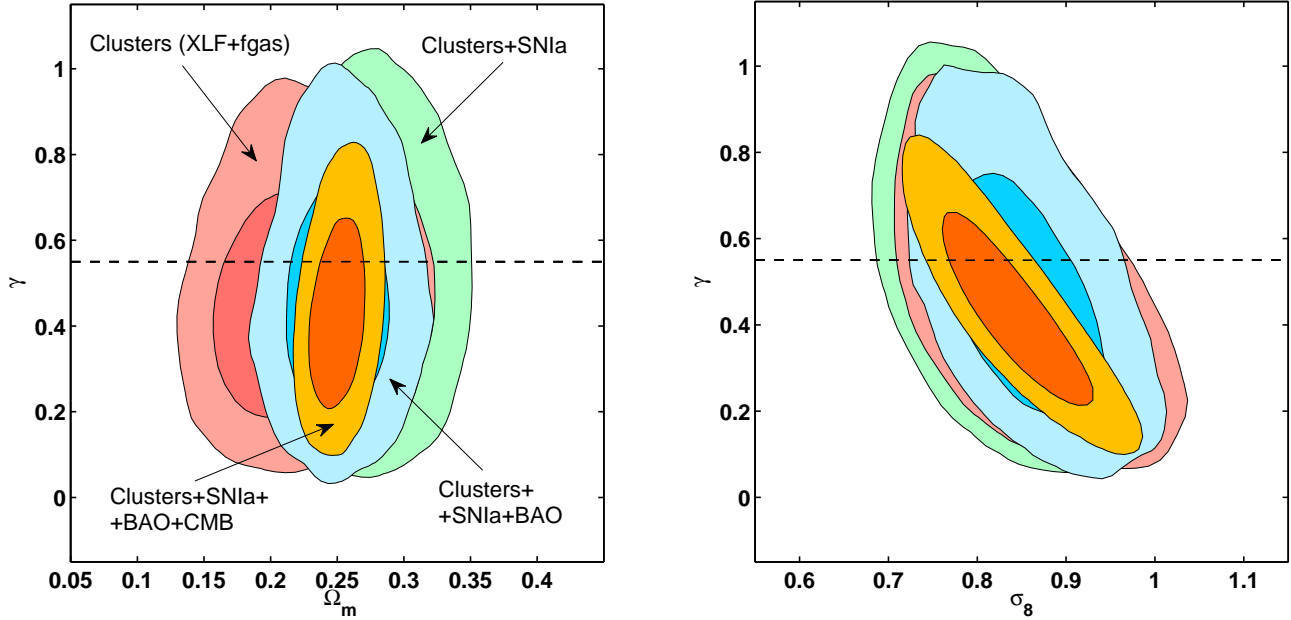


Figure 5. 68.3 and 95.4 per cent confidence contours in the Ω_m, γ (left panel) and σ_8, γ (right panel) planes for the flat Λ CDM background expansion with self-similar evolution and constant scatter in the scaling relations. Results are shown for the following combinations of data sets: XLF+ f_{gas} (red contours), XLF+ f_{gas} +SNIIa (green contours), XLF+ f_{gas} +SNIIa+BAO (blue contours), and XLF+ f_{gas} +SNIIa+BAO+CMB (gold, smallest contours). This figure does not include the additional constraints on γ from the ISW effect. The horizontal, dashed lines mark $\gamma = 0.55$ (GR).

Table 1. Marginalized 68.3 per cent confidence constraints for various subsets of the data, for the flat Λ CDM ($w = -1$) and flat w CDM (w constant) background expansion models. Note: ^athese results do not include the constraints on γ from the ISW effect.

Data	Ω_m	σ_8	$\beta_2^{\ell m}$	$\sigma'_{\ell m}$	w	γ
XLF+ f_{gas}	$0.214^{+0.036}_{-0.041}$	$0.85^{+0.07}_{-0.06}$	0	0	-1	$0.42^{+0.20}_{-0.16}$
XLF+ f_{gas} +SNIIa	$0.260^{+0.040}_{-0.025}$	$0.83^{+0.06}_{-0.07}$	0	0	-1	$0.43^{+0.25}_{-0.15}$
XLF+ f_{gas} +SNIIa+BAO	$0.247^{+0.028}_{-0.024}$	$0.85^{+0.05}_{-0.06}$	0	0	-1	$0.41^{+0.24}_{-0.15}$
XLF+ f_{gas} +SNIIa+CMB	$0.266^{+0.018}_{-0.021}$	$0.85^{+0.04}_{-0.06}$	0	0	-1	$0.40^{+0.15}_{-0.12}$
XLF+ f_{gas} +SNIIa+BAO+CMB ^a	$0.248^{+0.017}_{-0.012}$	$0.84^{+0.06}_{-0.06}$	0	0	-1	$0.42^{+0.15}_{-0.15}$
XLF+ f_{gas} +SNIIa+BAO+CMB	$0.249^{+0.015}_{-0.013}$	$0.84^{+0.05}_{-0.05}$	0	0	-1	$0.40^{+0.13}_{-0.12}$
"	$0.252^{+0.015}_{-0.014}$	$0.82^{+0.05}_{-0.05}$	$-0.36^{+0.44}_{-0.51}$	0	-1	$0.44^{+0.17}_{-0.13}$
"	$0.249^{+0.018}_{-0.010}$	$0.82^{+0.06}_{-0.04}$	0	$-0.52^{+0.35}_{-0.33}$	-1	$0.45^{+0.14}_{-0.13}$
"	$0.249^{+0.017}_{-0.011}$	$0.84^{+0.05}_{-0.06}$	$0.33^{+0.72}_{-0.76}$	$-0.82^{+0.57}_{-0.37}$	-1	$0.40^{+0.17}_{-0.13}$
"	$0.251^{+0.016}_{-0.014}$	$0.83^{+0.06}_{-0.04}$	0	0	$-0.98^{+0.07}_{-0.07}$	$0.39^{+0.14}_{-0.13}$

6.4 The impacts of the different data sets

The green, dotted-dashed line in Figure 4 shows the marginalized constraints on γ from the XLF data alone¹³.

¹³ Note that the XLF data include f_{gas} measurements for the six lowest redshift clusters in the sample of Allen et al. (2008), which serve to normalize the M_{gas} mass proxy (see details in Paper I). For the XLF data alone, we obtain the same constraints on γ and σ_8 than those from the XLF+ f_{gas} (full sample) data (see Table 1), and only ~ 10 weaker constraints on Ω_m .

The red, dashed line shows the constraints from the combination of SNIIa, f_{gas} , BAO, and CMB data, excluding the XLF. It is readily apparent that the constraints on γ from the combination of all other data sets, excluding the XLF, are significantly weaker than those from the XLF data alone. Without the XLF data, the constraints on γ are primarily provided by the ISW effect, and we obtain $\gamma = 0.38^{+0.23}_{-0.69}$. Combining the XLF and other data, we obtain the blue, solid curve and constraints on γ more than three times tighter than without the XLF (see Table 1).

Although the XLF data dominate the constraints on γ ,

the other data (f_{gas} , SNIa, BAO, and CMB) provide complementary information on other cosmological parameters. These additional constraints break degeneracies with γ and help to exploit fully the ability of the XLF data to constrain γ . To demonstrate the impacts of these data sets, Figure 5 shows the constraints in the Ω_m, γ (left panel) and σ_8, γ (right panel) planes for various subsets of data. The red contours show the constraints from the XLF+ f_{gas} data (i.e. only cluster data); the green contours show the results from adding SNIa data (i.e. XLF+ f_{gas} +SNIa); the blue contours from adding BAO to the rest; and the gold (smallest) contours from adding CMB data¹⁴.

The left panel of Figure 5 demonstrates again the absence of any strong correlation between Ω_m and γ (see also Section 6.1). These results (see also Table 1) show that simply improving our knowledge of Ω_m , and therefore the expansion history (by e.g. adding BAO to XLF+ f_{gas} +SNIa data), will not necessarily improve the constraints on γ .

The right panel of Figure 5 shows the constraints in the σ_8, γ plane. We see that the combination of the CMB data with the other data sets considerably strengthens the correlation between these parameters. The reason for this is that the inclusion of the CMB data significantly reduces the range of allowed values not only for the expansion history but also for other relevant cosmological parameters, placing tight constraints on, e.g., $\Omega_b h^2$, $\Omega_c h^2$, n_s , τ , H_0 , and A_s . These constraints lead to a tight constraint on $\sigma_8(z)$ at early times ($z \sim 1100$), where GR is assumed (i.e., $z > z_t$).

7 CONCLUSIONS

We have used measurements of the evolution of massive galaxy clusters from wide-area X-ray cluster surveys (spanning the redshift range $z < 0.5$), and simultaneous measurements of the observable-mass scaling relations, to test the consistency of the observed growth rate of clusters with that predicted for GR. We allow departures from GR as described by the parameterization $\Omega_m(z)^\gamma$, for which $\gamma \sim 0.55$ corresponds to GR. We find that the current data are consistent with GR and give tight constraints on departures from it. Assuming constant scatter and purely self-similar evolution of the cluster observable-mass scaling relations, and a flat Λ CDM background evolution model, the combination of XLF, f_{gas} , SNIa, BAO, and CMB data gives $\gamma(\sigma_8/0.8)^{6.8} = 0.55^{+0.13}_{-0.10}$. Allowing w to vary, we simultaneously demonstrate consistency with the expansion history of Λ CDM (i.e. $w = -1$).

Our analysis employs the method described in Paper I, which self-consistently models X-ray cluster survey data and follow-up observations to simultaneously constrain both cosmological and scaling relation parameters. This allows us to constrain γ even when allowing for departures from self-similar evolution and/or constant scatter in the luminosity-mass relation. We caution that the adoption of such a self-

consistent approach to model the survey+follow-up data is important, else spuriously tight, and potentially biased, constraints may be obtained.

Our measurements of the growth of the most X-ray luminous, most massive galaxy clusters within $z < 0.5$ constrain the growth of cosmic structure during the epoch of cosmic acceleration. It is primarily this redshift dependence that provides our constraints on γ , although we have also utilized the small contribution from the ISW effect, which probes larger scales at $z < 2$. The inclusion of CMB and other data tightens significantly the constraints on the background expansion model and other cosmological parameters leading to a clear correlation between γ and σ_8 . This highlights the potential for further improvements in γ with the incorporation of precise, independent measurements of σ_8 .

ACKNOWLEDGMENTS

We thank A. Lewis, M. Amin, R. Blandford, and R. Wagner for useful discussions. We thank G. Morris for technical support. The computational analysis was carried out using the KIPAC XOC and Orange computer clusters at SLAC. We acknowledge support from the National Aeronautics and Space Administration (NASA) through LTSA grant NAG5-8253, and through Chandra Award Numbers DD5-6031X, GO2-3168X, GO2-3157X, GO3-4164X, GO3-4157X, GO5-6133, GO7-8125X and GO8-9118X issued by the Chandra X-ray Observatory Center, which is operated by the Smithsonian Astrophysical Observatory for and on behalf of the NASA under contract NAS8-03060. This work was supported in part by the U.S. Department of Energy under contract number DE-AC02-76SF00515. AM was supported by a Stanford Graduate Fellowship and an appointment to the NASA Postdoctoral Program, administered by Oak Ridge Associated Universities through a contract with NASA.

REFERENCES

- Adelman-McCarthy J. K. et al., 2007, ApJ S., 172, 634
- Allen S. W., Rapetti D. A., Schmidt R. W., Ebeling H., Morris R. G., Fabian A. C., 2008, MNRAS, 383, 879
- Allen S. W., Schmidt R. W., Ebeling H., Fabian A. C., van Speybroeck L., 2004, MNRAS, 353, 457
- Astier P. et al., 2006, Astron. Astrophys., 447, 31
- Barris B. J. et al., 2004, ApJ, 602, 571
- Böhringer H. et al., 2004, Astron. Astrophys., 425, 367
- Bond J. R., Cole S., Efstathiou G., Kaiser N., 1991, ApJ, 379, 440
- Bryan G. L., Norman M. L., 1998, Astrophys. J., 495, 80
- Cabre A., Gaztanaga E., Manera M., Fosalba P., Castander F., 2006, Mon. Not. Roy. Astron. Soc. Lett., 372, L23
- Challinor A., Lasenby A., 1999, ApJ, 513, 1
- Chan K. C., Scoccimarro R., 2009, Phys. Rev.D, 80, 104005
- Chiang H. C. et al., 2010, ApJ, 711, 1123
- Cohn J. D., White M., 2008, MNRAS, 385, 2025
- Colless M. et al., 2001, MNRAS, 328, 1039
- Colless M. et al., 2003, astro-ph/0306581

¹⁴ Since, for this figure, we are primarily interested in the ability of the CMB data to improve our knowledge of γ by constraining other cosmological parameters, we do not include the additional constraining power on γ from the ISW effect (i.e. we assume that for the large scales relevant for the ISW, GR is recovered). This has only a small impact on the results (see R09 and Table 1).

- Copeland E. J., Sami M., Tsujikawa S., 2006, *International Journal of Modern Physics D*, 15, 1753
- Daniel S. F., Linder E. V., Smith T. L., Caldwell R. R., Cooray A., Leauthaud A., Lombriser L., 2010, arXiv:1002.1962
- Di Porto C., Amendola L., 2008, *Phys. Rev.*, D77, 083508
- Dunkley J. et al., 2009, *ApJ S.*, 180, 306
- Dvali G., Gabadadze G., Porrati M., 2000, *Physics Letters B*, 485, 208
- Ebeling H., Edge A. C., Bohringer H., Allen S. W., Crawford C. S., Fabian A. C., Voges W., Huchra J. P., 1998, *MNRAS*, 301, 881
- Ebeling H., Edge A. C., Henry J. P., 2001, *ApJ*, 553, 668
- Eisenstein D. J. et al., 2005, *ApJ*, 633, 560
- Evrard A. E. et al., 2002, *ApJ*, 573, 7
- Fosalba P., Gaztanaga E., Castander F., 2003, *ApJ*, 597, L89
- Francis M. J., Lewis G. F., Linder E. V., 2009, *MNRAS*, 394, 605
- Freedman W. L. et al., 2001, *ApJ*, 553, 47
- Frieman J. A., Turner M. S., Huterer D., 2008, *ARA&A*, 46, 385
- Gannouji R., Polarski D., 2008, *JCAP*, 0805, 018
- Garnavich P. M. et al., 1998, *ApJ*, 509, 74
- Giannantonio T., Scranton R., Crittenden R. G., Nichol R. C., Boughn S. P., Myers A. D., Richards G. T., 2008, *Phys. Rev.D*, 77, 123520
- Grossi M., Springel V., 2009, *MNRAS*, 394, 1559
- Gupta S. et al., 2009, arXiv:0909.1621
- Hicken M., Wood-Vasey W. M., Blondin S., Challis P., Jha S., Kelly P. L., Rest A., Kirshner R. P., 2009, *ApJ*, 700, 1097
- Ho S., Hirata C., Padmanabhan N., Seljak U., Bahcall N., 2008, *Phys. Rev.D*, 78, 043519
- Hu W., 2005, *Phys. Rev.*, D71, 047301
- Hu W., 2008, *Phys. Rev.*, D77, 103524
- Hu W., Sawicki I., 2007, *Phys. Rev.*, D76, 104043
- Huterer D., Linder E. V., 2007, *Phys. Rev.*, D75, 023519
- Jenkins A., Frenk C. S., White S. D. M., Colberg J. M., Cole S., Evrard A. E., Couchman H. M. P., Yoshida N., 2001, *MNRAS*, 321, 372
- Jennings E., Baugh C. M., Angulo R. E., Pascoli S., 2010, *MNRAS*, 401, 2181
- Jones W. C. et al., 2006, *ApJ*, 647, 823
- Kaiser N., 1986, *MNRAS*, 222, 323
- Kirkman D., Tytler D., Suzuki N., O'Meara J. M., Lubin D., 2003, *ApJ S.*, 149, 1
- Klypin A., Maccio A. V., Mainini R., Bonometto S. A., 2003, *Astrophys. J.*, 599, 31
- Knop R. A. et al., 2003, *ApJ*, 598, 102
- Komatsu E. et al., 2009, *ApJ S.*, 180, 330
- Kosowsky A., Milosavljevic M., Jimenez R., 2002, *Phys. Rev.*, D66, 063007
- Kowalski M. et al., 2008, *ApJ*, 686, 749
- Kuhlen M., Strigari L. E., Zentner A. R., Bullock J. S., Primack J. R., 2005, *MNRAS*, 357, 387
- Lewis A., Bridle S., 2002, *Phys. Rev.D*, 66, 103511
- Linder E. V., 2005, *Phys. Rev.*, D72, 043529
- Linder E. V., Cahn R. N., 2007, *Astropart. Phys.*, 28, 481
- Linder E. V., Jenkins A., 2003, *MNRAS*, 346, 573
- Lokas E. L., Bode P., Hoffman Y., 2004, *MNRAS*, 349, 595
- Lukić Z., Heitmann K., Habib S., Bashinsky S., Ricker P. M., 2007, *ApJ*, 671, 1160
- Maccio A. V., Quercellini C., Mainini R., Amendola L., Bonometto S. A., 2004, *Phys. Rev.*, D69, 123516
- Mainini R., Maccio A. V., Bonometto S. A., 2003, *New Astron.*, 8, 173
- Mantz A., Allen S. W., Ebeling H., Rapetti D., 2008, *MNRAS*, 387, 1179
- Mantz A., Allen S. W., Rapetti D., Ebeling H., 2009a, arXiv:0909.3098 (Paper I)
- Mantz A., Allen S. W., Ebeling H., Rapetti D., Drlica-Wagner A., 2009b, arXiv:0909.3099 (Paper II)
- Mota D. F., Kristiansen J. R., Koivisto T., Groeneboom N. E., 2007, *Mon. Not. Roy. Astron. Soc.*, 382, 793
- Nesseris S., Perivolaropoulos L., 2008, *Phys. Rev.*, D77, 023504
- Peebles P. J. E., 1980, *The large-scale structure of the universe*. Princeton University Press, 1980.
- Percival W. J., Cole S., Eisenstein D. J., Nichol R. C., Peacock J. A., Pope A. C., Szalay A. S., 2007, *MNRAS*, 381, 1053
- Percival W. J. et al., 2010, *MNRAS*, 401, 2148
- Perlmutter S. et al., 1999, *ApJ*, 517, 565
- Press W. H., Schechter P., 1974, *ApJ*, 187, 425
- Rapetti D., Allen S. W., Mantz A., Ebeling H., 2009, *MNRAS*, 400, 699 (R09)
- Rapetti D., Allen S. W., Weller J., 2005, *MNRAS*, 360, 555
- Readhead A. C. S. et al., 2004, *Science*, 306, 836
- Reed D. S., Bower R., Frenk C. S., Jenkins A., Theuns T., 2007, *MNRAS*, 374, 2
- Reichardt C. L. et al., 2009, *ApJ*, 694, 1200
- Reyes R., Mandelbaum R., Seljak U., Baldauf T., Gunn J. E., Lombriser L., Smith R. E., 2010, *Nature*, 464, 256
- Riess A. G. et al., 1998, *AJ*, 116, 1009
- Riess A. G. et al., 2007, *ApJ*, 659, 98
- Riess A. G. et al., 2004, *ApJ*, 607, 665
- Sapone D., Amendola L., 2007, arXiv:0709.2792
- Schmidt B. P. et al., 1998, *ApJ*, 507, 46
- Schmidt F., 2009a, *Phys. Rev.D*, 80, 043001
- Schmidt F., 2009b, *Phys. Rev.D*, 80, 123003
- Schmidt F., Lima M., Oyaizu H., Hu W., 2009, *Phys. Rev.D*, 79, 083518
- Schrabback T. et al., 2009, arXiv:0911.0053
- Scranton R. et al., 2003, astro-ph/0307335
- Sheth R. K., Tormen G., 1999, *MNRAS*, 308, 119
- Spergel D. N. et al., 2007, *ApJ S.*, 170, 377
- Spergel D. N. et al., 2003, *ApJ S.*, 148, 175
- Spiegelhalter D. J., Best N. G., Carlin B. P., van der Linde A., 2002, *J. Roy. Statist. Soc. B*, 64, 583
- Tinker J., Kravtsov A. V., Klypin A., Abazajian K., Warren M., Yepes G., Gottlöber S., Holz D. E., 2008, *ApJ*, 688, 709
- Tonry J. L. et al., 2003, *ApJ*, 594, 1
- Vikhlinin A. et al., 2009, *ApJ*, 692, 1060
- Wang L.-M., Steinhardt P. J., 1998, *Astrophys. J.*, 508, 483
- Wei H., 2008, *Phys. Lett.*, B664, 1
- Weller J., Lewis A. M., 2003, *MNRAS*, 346, 987
- White S. D. M., Navarro J. F., Evrard A. E., Frenk C. S., 1993, *Nat*, 366, 429
- Wood-Vasey W. M. et al., 2007, *ApJ*, 666, 694
- Zhao G., Giannantonio T., Pogosian L., Silvestri A., Ba-

con D. J., Koyama K., Nichol R. C., Song Y., 2010,
arXiv:1003.0001